



A mesomechanical approach to inhomogeneous particulate composites undergoing localized damage: part I—a mesodomain simulation

Chingshen Li, F. Ellyin*

Department of Mechanical Engineering, University of Alberta, Edmonton, T6G 2G8, Canada

Received 6 November 1997; in revised form 15 October 1998

Abstract

This paper presents a mesoscale homogenization methodology to deal with the damage localization in inhomogeneous particulate-reinforced composites. An effective local particle volume fraction, $f_{loc,eff}^v$, which includes the particle size effect is suggested to characterize the damage-inducing aspect of clusters. The clustering regions in a particulate composite accommodating the saturated local damage at an applied stress amplitude are simulated by mesodomains, subdomains of homogeneous medium and homogeneous damage distribution. The size of the mesodomains is determined by the transition condition from local damage to global damage via macro-mechanics. The mesodomain positions are found in a materials science manner by mapping the 'area contours' of $f_{loc,eff}^v$ for the composite. Transformation of a clustering composite into a two-homogeneous phase material enables one to appropriately illustrate the local constitutive behaviours, and paves the way to predict saturated local damage life. © 1999 Elsevier Science Ltd. All rights reserved.

1. Introduction

Inhomogeneous microstructures in metals and alloys, as well as in other engineering materials, have been neglected by solid mechanics which, in most cases, efficiently simplifies structural design and benefits the end-users of the materials (Bazant, 1997). This traditional simplification method is increasingly challenged in the particulate and short fibre reinforced composites, where the scale of reinforcement inhomogeneity is large and the degree of induced damage localization is high.

The scale of the inhomogeneous reinforcement distribution, or clusters, ranges from a few dozen microns to about 1 mm in the extruded particle-reinforced metal matrix composites (PMMCs), which is the focus of this study (Davidson, 1991). This scale, termed mesoscale, is an intermediate one between the micro scale, the size of particles, and the macroscale of an overall component.

* Corresponding author. Tel.: 001 403 492 2009; fax: 001 403 492 2200

Mesoscale and microscale have been referred to as laminae and fibers, respectively, for polymer matrix composites (Ladeveze et al., 1993). The difference between these two cases is that laminae are mesoscale material constituents of polymer composites, while clusters are, more or less, mesoscale defects of PMMCs.

It is increasingly evident that meso-structures play a prominent role in influencing mechanical behaviour and inducing localized damage in composites. It is found that particle clusters considerably reduce the ductility of the materials under monotonic loading, however the yield stress is not notably reduced (Lloyd, 1995; Lewandowski et al., 1989). Microscopic observation shows that the monotonic loading-induced final fracture initiates from one of the clusters and passes through others (Brockenbrough et al., 1992). Finite element analysis by Christman et al. (1989) indicates that clustering tends to reduce the flow stress of PMMCs. Under cyclic loading particle–matrix interface debonding, particle fracture and short cracks typically initiate in the clustering regions (Li and Ellyin, 1996). Consequently, damage localization occurs in PMMCs.

Significant effort has been devoted to understanding the inhomogeneity-induced damage that violates the basic assumptions of continuum mechanics and continuum damage mechanics (Kachanov, 1958; Chaboche, 1988). Lemaitre (1986) pointed out that it requires a discontinuous variable to model the high degree of damage localization. Modelling the broken and intact particles as homogeneous damaged cells and undamaged cells, respectively, Maire et al. (1997) applied the self-consistent method to predict the tensile behaviour of PMMCs. However, the role of clusters in inducing localized strain and damage has not been addressed. Simple modelling of materials and damage distributions can be effective in clarifying some aspects of the physics of damage evolution (Iwan, 1967), provided the following issues can be properly addressed: At what scale are the materials homogenized? What purposes do the models serve? What methods homogenize?

The present study aims at developing a local homogenization methodology so that a local damage law can be derived and the saturated local damage life can be predicted for the clustering particulate composite. This study focusses on the clustering regions of a critical mesoscale, at which the local damage is saturated under a specific loading level for a specific fatigue life or creep time. This mesodomain simulation combines approaches of solid mechanics and materials science, which are applied to determine the size and positions of the mesodomains in the composite, respectively.

2. Clusters and effective local particle volume fraction

Clustering of particles in PMMCs is inevitable due to the manufacturing process of the composites. A typical clustering of particles in an extruded alumina reinforced 6061 aluminum alloy ($\text{Al}_2\text{O}_3/6061\text{Al}$) under T6 heat-treatment is shown in Fig. 1. This material was produced by Duralcan, a subsidiary of Alcan International Ltd. The average particle size of the material is $12\ \mu\text{m}$ and the global volume fraction of particles is 20%. The micrograph in Fig. 1 shows one large cluster and two small clusters of higher local volume fraction of particles.

Considerable effort has been made to measure and characterize particle cluster distributions in PMMCs, although there is no established standard to do so. Quantitative image analysis has been the most popular tool to examine particle distribution (Pilkey et al., 1990). The particle size and particle volume fraction in clusters can also be statistically measured and analysed using digital

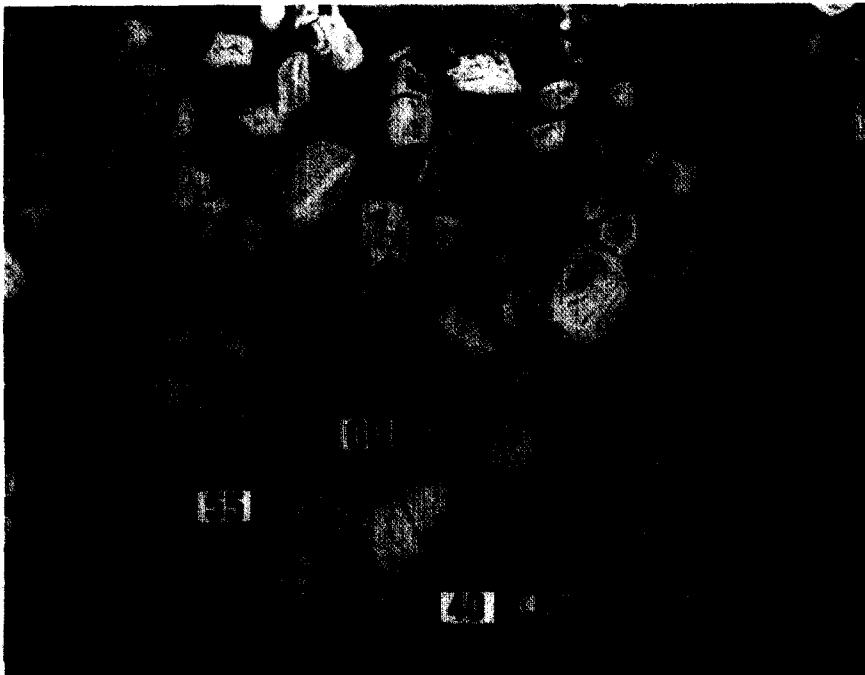


Fig. 1. Clustering distribution and localized damage in 20% average volume fraction $\text{Al}_2\text{O}_3/6061$ Al after 10^5 cycles of $\sigma_{\max} = 210$ MPa, $R = -0.35$. The numbers on the circles indicate the effective local particle volume fraction inside the area.

microscopic imaging systems and software. Pilkey et al. (1990) have suggested inter-particle dilational spacing (IPDS) as a description of clustering distribution in PMMCs. Local volume fraction of particles is also used to show the clustering of particles (Brockenbrough et al., 1992). Since particle size and shape in a cluster also affect the local stress, strain and local damage development, a single measure of local volume fraction cannot characterize the cluster's possibility of inducing localized damage. Moreover, the particle distance beneath the surface would be considerably different from the IPDS value measured on the specimen surface.

Several comparative experiments conducted on the effect of average volume fraction and average particle size on the mechanical behaviour of PMMCs may shed light on the investigation of local parameters of clusters. It is found that for a series of composites having the same average particle size but different particle volume fraction, the elastic modulus increases, while fracture toughness K_{Ic} (Flom and Arsenault, 1989), elongation and ductility (Mummery and Derby, 1991; Lloyd, 1995) decrease with an increase of the particle volume fraction. On the other hand, for composites with constant particle volume fraction, ductility, cracked particle density (Lloyd, 1995), and fracture toughness (Flom and Arsenault, 1989) decrease with an increase of the average particle size. The damage in clusters results from the clustering-induced high local stress—hydrostatic stress—(Pragnell et al., 1996). These results suggest that a high local volume fraction causes a local stress-strain concentration and plays an important role in inducing damage. However, the effect of average local particle size is not negligible.

To characterize clusters, especially regarding their damage inducing prospects, an effective local volume fraction of particles is proposed that includes the size effect of the largest particles in the cluster. The particle shape is assumed to be statistically the same in the clusters as in the surrounding domains. The effective local volume fraction, $f_{loc,eff}^v$, is then defined as

$$f_{loc,eff}^v = f_{loc}^v + \alpha(d_{loc}^n - d_c^n) \quad (1)$$

in which d_c and d_{loc} are the average particle size for the composite and the cluster, respectively, while α and n are constants which depend on the composite constituents and the temperature of PMMCs. As temperature increases, the matrix constraint for plastic deformation and residual stress will change, therefore the damage prospects of the cluster will change. Based on the comparative experimental results (Flom and Arsenault, 1989), it is estimated that n is approximately equal to 1, and $\alpha = 0.018/\text{micron}$. That is, a 10-micron increase of the average particle size results in a 1.8% volume fraction increase with regards to inducing damage. The $f_{loc,eff}^v$ weighs the local volume fraction of a cluster of particles with the local average particle size in the cluster. It can be measured and calculated area by area with the assistance of quantitative image techniques.

The following procedures are applied in this study to reveal and display the clustering distribution in a particulate composite. As the first step, a histogram of local particle volume fraction of the composite is measured and serves as an indicator of clustering distribution. The particle area fraction measured on the specimen surface is statistically approximately equal to the volume fraction. As an example, a histogram of local volume fraction in the mesodomains of $10,000 \mu\text{m}^2$ in area, in a 20% volume fraction with $12 \mu\text{m}$ average particle size composite, is shown in Fig. 2. If the subdomain area is increased, the fraction of the subdomains having the global average volume fraction increases. The divergence of local particle volume fraction from the average, or presence of a certain percentage of volume fractions, which are considerably higher or lower than

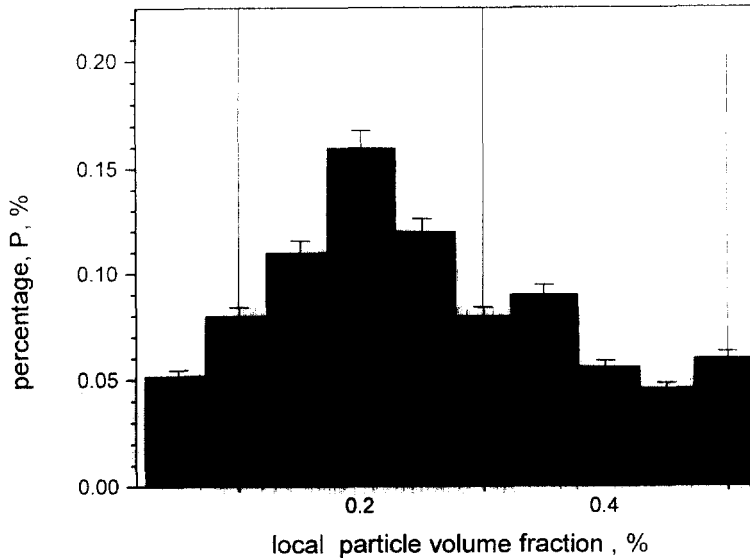


Fig. 2. A histogram of local particle volume fraction distribution in an $\text{Al}_2\text{O}_3/6061$ Al composite.

the global average particle volume fraction, is an indicator of the cluster distribution of particles.

Secondly, 'area contours' of the effective local particle volume fraction are suggested to show the clustering regions and degree of clustering. These contours display the boundaries of areas of the same $f_{\text{loc,eff}}^v$ value. Circles are chosen to show the contour regions for the extruded PMMCs. Although other shapes, such as ellipsoid, can be applied, the sphere shape provides reasonable approximation to the real shape of clusters in extruded PMMCs and considerable convenience in calculating the local stress-strain, which will be shown in Part II. The minimum area diameter is found to be approximately four times larger than the average particle size, according to statistical experimental observation. For this $\text{Al}_2\text{O}_3/6061$ composite, it is about 50 microns. It is noteworthy that these $f_{\text{loc,eff}}^v$ 'contours' are different from stress and strain contours. The 'area contours' for the particle distribution are also shown in Fig. 1. The larger outside area contour's $f_{\text{loc,eff}}^v$ is 40%, while $f_{\text{loc,eff}}^v$ for the two small regions is 55 and 60%, respectively. Note that while $f_{\text{loc,eff}}^v$ is measured and displayed in two dimensions, it nevertheless represents three-dimensional events statistically. For example, a circle area contour may be envisaged to represent an intersection of a sphere with a plane.

Finally, a representative area contour plot of $f_{\text{loc,eff}}^v$, determined from a typical and large enough micrograph, is suggested to show the clustering morphology of a composite. This micrograph should contain the same percentage of larger clusters and the same morphology of cluster distribution as the whole material. In other words, this micrograph represents the mesoscale structure pattern of a representative volume element of the composite (Bazant, 1997).

The procedures quantitatively characterize the clustering distribution which induces damage localization in the particulate composites.

3. Damage localization and globalization

3.1. Phenomena of damage localization

The damage process of heterogeneous engineering materials is divided into two stages: (1) damage localization stage and (2) damage globalization stage, based on the assumption that the physical damage process is solely dependent on the applied stress–strain. The termination of localized damage can be caused by the increase of loading level (monotonic), load cycles (fatigue) or loading times (creep).

Monotonic loading-induced particle fracture and debonding are generally localized in the particle clusters of PMMCs. A tensile test using PMMC specimens with electro-etched circles shows considerably higher strain in some clustering regions, and micro cracks initiate from these locations (Lloyd, 1991). These micro cracks coalesce resulting in final fracture as the applied stress approaches fracture stress (Brockenbrough et al., 1992).

Fatigue tests have shown that particle debonding, particle fracture and short crack growth usually occur in the clustering ranges in the early stages of cyclic loading (Li and Ellyin, 1996). This feature is also shown in Fig. 1, which was taken after 1.0×10^5 cycles under $\sigma_{\max} = 210$ MPa, $R = -0.35$. The top part of Fig. 3 schematically displays a typical crack (flaw) growth pattern in PMMCs under constant cyclic loading. A short crack initiates and grows in a cluster with fractured and debonded particles. The short crack growth rate changes dramatically at constant cyclic stress. As loading cycles continue, a long crack is formed which has a growth rate resembling the Paris law (see the lower plot in Fig. 3). During the long crack growth, the damaged clusters on the path will not affect crack growth rate and direction (Li and Ellyin, 1996).

The above experimental observation has shown that the damage localization stage of PMMCs includes particle fracture, debonding and short crack growth in clusters. The second stage, the damage globalization stage, consists of long crack growth under cyclic loading or void coalescence under monotonic loading. The localized damage is strongly dependent on the local structure in the clusters, while the second stage is governed by the global stress field and can be adequately described by linear elastic fracture mechanics (Shang and Ritchie, 1988).

3.2. Scale of saturated local damage

Considerable effort during the past two decades has reached the consensus that short cracks are microstructure sensitive, and that their growth is influenced by local microstructures (Kitagawa and Takahashi, 1976). From the damage mechanics point of view, short crack initiation and growth is a localized damage process while long crack growth is a damage globalization process. Linear elastic fracture mechanics can be applied for the latter, but not for short crack growth. A successful solution for the prediction of the entire damage process depends on prediction of local damage saturation, or the transition from small crack to long crack growth.

The transition condition from localization to globalization can be found from a crack diagram showing the flaw (crack) size versus applied stress, Fig. 4. The K_{th} line in the diagram is similar to the Kitagawa–Takahashi diagram (1976). This Figure is a replot of our previous crack phase diagram in a log–log scale (Li and Ellyin, 1995a). The short crack growth (SG) phase coincides with the localized damage zone, while pre-cessation short crack growth (PCS) phase refers to the

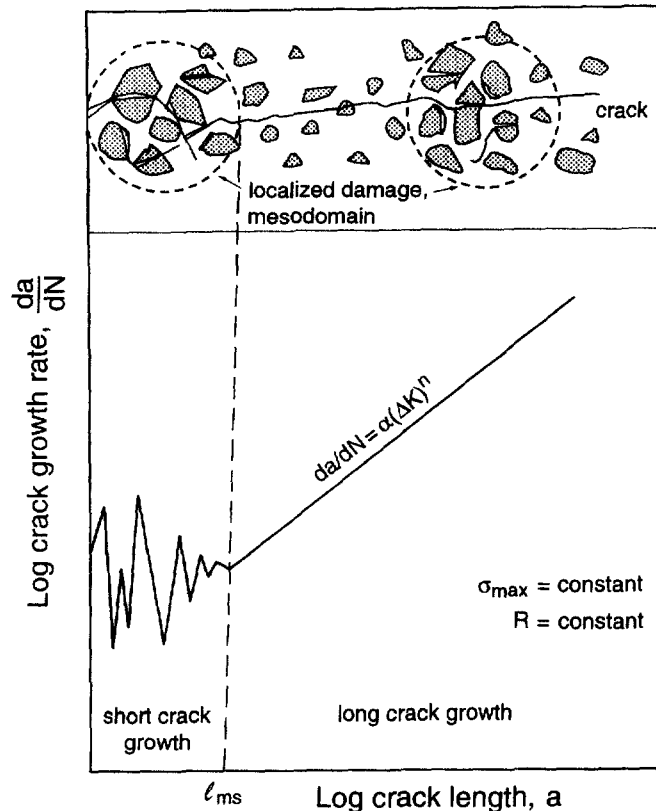


Fig. 3. Comparison of crack growth rate and growth pattern in the damage localization stage with that in the damage globalization stage under constant cyclic stress.

permanently localized damage zone. The hk line represents the transition from damage localization to long crack growth.

To rationalize both long and short crack growth behaviour, El Haddad et al. (1979) proposed an expression of the stress intensity factor as

$$\Delta K = C_2 \Delta \sigma \sqrt{\pi(a + a_0)} \quad (2)$$

in which a_0 was referred to as an intrinsic crack length, although its physical meaning for metals is still in dispute (Suresh and Ritchie, 1984). From the damage mechanics point of view, a_0 is an intrinsic material scale, which represents an equivalent crack length for the saturated local damage zone. Hence, the above equation is applied in this study to determine the scale of saturated damage localization at the fatigue limit and fracture stress.

In the near threshold and fatigue limit region, a_0 corresponds to the intersection point of the extended straight line of the Paris law of constant K_{th} with the fatigue limit line in the Kitagawa–Takahashi plot. There are a number of experimental data which show an agreement with eqn (2) e.g. (Liu and Liu, 1982). In PMMCs short cracks grow much longer with greater sensitivity to the

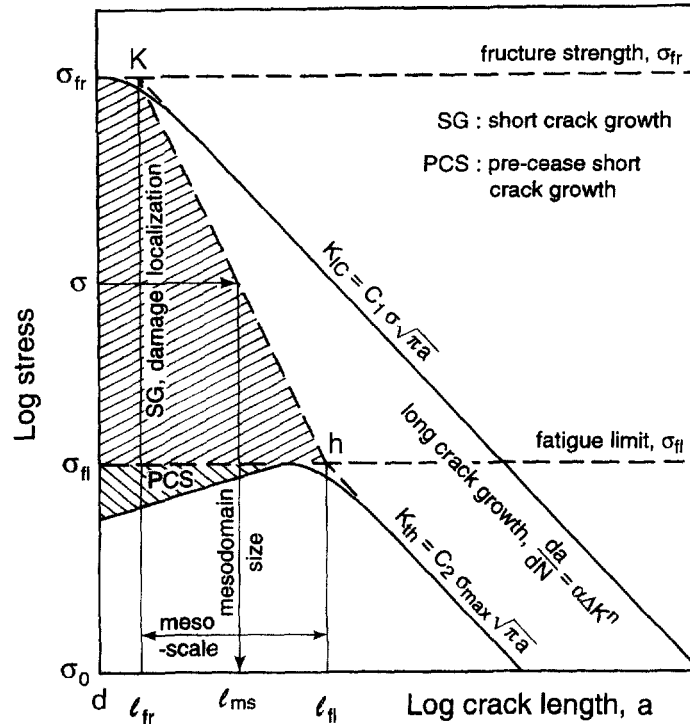


Fig. 4. An applied stress-crack length plot in log–log scales showing the localized damage zone.

local structure than in metals. Assuming $a_0 = l^n$ when $a = 0$ in eqn (2), then l^n will correspond to the crack length of point h in Fig. 4, and it is given by

$$l^n = \frac{K_{Ih}^2}{Y\pi\sigma_n^2} \tag{3}$$

in which σ_n is the fatigue limit of the material. As shown in Fig.4, l^n is an intersection point of the extended threshold condition line with the fatigue limit line. Thus, l^n represents the largest clustering region accommodating the saturated local damage.

The size of flaw where fracture originates under monotonic loading is related to the fracture strength of the material (Hoshide et al., 1984). The size which leads to rupture of PMMCs under fracture stress can be determined in a manner similar to eqn (3),

$$l^{fr} = \frac{K_{IC}^2}{Y\pi\sigma_f^2} \tag{4}$$

where K_{IC} is the fracture toughness and σ_f is the fracture stress of the material. The flaw size from which the fracture may originate corresponds to point K in Fig. 4. For PMMCs, l^{fr} corresponds to the smallest clustering area of the highest $f_{loc,eff}^v$. It is worth noting that l^{fr} is considerably larger than the flaw size in metals and ceramics (Hoshide, 1995). These size characteristics can be found

in the fractograph of fractured samples of PMMCs under monotonic loading. For example, in alumina reinforced 6061 alloys, l^{fr} and l^n are about 60 and 1000 μm , respectively.

Thus, l^n and l^{fr} represent the upper and lower bounds of damage localization, and can be viewed as parameters characterizing materials. As shown in Fig. 4, at the intermediate range, the transition from localized damage to long crack growth occurs at a flaw size of l_{ms} . l_{ms} is also used to determine the size of local homogenized subdomains for the clusters.

4. Mesodomain simulation of clustering regions with localized damage

4.1. Concept of mesodomains

Experimental observation indicates that damage tends to be localized at the clustering regions of higher value, $f_{loc,eff}^v$ in PMMCs at an early stage of cyclic loading (Li and Ellyin, 1995). To simplify the complicated local particle distribution pattern and local damage variation in the clustering regions of PMMCs, these regions are simulated by mesodomains, subdomains of a homogeneous medium and homogeneously distributed damage. Meanwhile, the remaining domains form a ‘matrix’, a homogeneous medium but free of damage in the early loading stage, i.e. the localized damage stage. This simulation transforms the inhomogeneous particulate composites undergoing localized damage into a homogeneous two phase ‘material’ of mesodomains and ‘matrix’, respectively.

Simulation of a particle clustering region in a PMMC under an applied stress level via a mesodomain is based on two criteria: (a) the size of the region is the same as the transition length, l_{ms} , from short crack growth to long crack growth, and (b) $f_{loc,eff}^v$ of this region is the maximum value among the same size subdomains. These are the ‘mechanics criterion’ and ‘material criterion’ of mesodomains.

The mesodomain size, by the first criterion, refers to the initial length of a crack transferring from short crack growth to LEFM dominated long crack growth. The line hk in Fig. 4 links the ‘inner’ flaw length at fracture stress and fatigue limit, and represents the boundary between the short crack phase and long crack phase of PMMCs (Li and Ellyin, 1995b). The mesodomain size, l_{ms} , can be obtained from the geometric relationship in Fig. 4,

$$\log l_{ms} = \log l^{fr} + \frac{\log \sigma_{fr} - \log \sigma}{\log \sigma_{fr} - \log \sigma_{fl}} (\log l^n - \log l^{fr}) \quad (5)$$

After the mesodomain size, l_{ms} , is determined through the framework of fracture mechanics, eqn (5), all mesodomains can be identified by mapping in the $f_{loc,eff}^v$ area contour plot as follows. The first part of the procedure is to find all the areas of the same diameter as l_{ms} in the contour plot of a representative area of the material. Secondly, the mesodomains are those subdomains with the maximum $f_{loc,eff}^v$ value. The maximum $f_{loc,eff}^v$ value of a subdomain causes the highest local stress concentration in the domain in comparison with the same size subdomains, hence the subdomain has the highest potential for damage under an applied stress. Figure 5 schematically displays the transformation of a cluster shown in the bottom micrograph into a mesodomain. The area contours

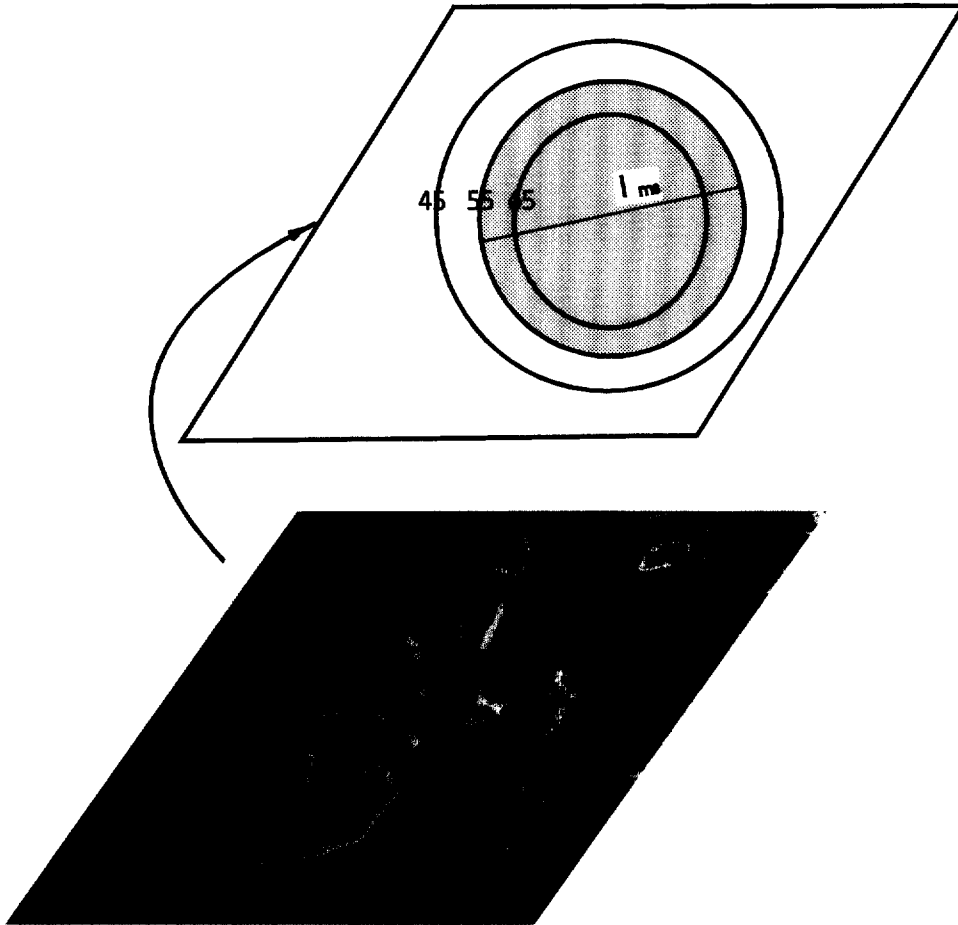


Fig. 5. Two criteria of mapping of an area contour circle into a mesodomain: the diameter of the circle is the same as the damage localization size, l_{ms} , and $f_{loc,eff}^y$ of the circle is the maximum among this size area contour circles.

for the cluster are approximate concentric circles. The circle with $f_{loc,eff}^v = 55\%$ has the same diameter as l_{ms} , and the contour value is the maximum for the same size subdomains.

Via this mesodomain simulation, the localized damage process is represented in the variation of local damage factor, D_{ms} , from 0 to 1. Analogous to the damage factor of the continuum damage mechanics, D_{ms} denotes the loss of effective area in the clustering region. One can then determine the correlation of local average stress, σ_{ms} , with the local damage factor as follows:

$$\sigma_{ms} = \frac{\sigma_{ms}^o}{1 - D_{ms}} \tag{6}$$

where σ_{ms}^o is the initial average local stress in the clustering region. When $D_{ms} = 1$, a long crack will form, and the above equation does not apply. $D_{ms} = 1$ also refers to saturation of localized damage. During the global damage stage when a long crack grows, $D_{ms} = 1$ will not change. This process is governed only by the global mechanics parameters, schematically shown in Fig. 3.

It is noteworthy that the size of mesodomains, into which clustering regions are to be simulated, depends on the applied stress level. Under a higher applied stress amplitude, a mesodomain occupies a smaller core-clustering with a higher $f_{loc,eff}^v$. Conversely, as the applied cyclic stress amplitude decreases, both the size and the saturation time (loading cycles) of the localized damage increases; thus, a mesodomain occupies a larger region of the same cluster. This is correlated with the size dependency of the ‘saturated local damage area’ on the applied stress level (Li and Ellyin, 1996).

4.2. Definition of the ‘matrix’

After the mesodomains are determined, the remaining subdomains of smaller $f_{loc,eff}^v$ value will become the ‘matrix’. During this transition the composite can be viewed as a two phase material of mesodomains and the ‘matrix’.

As an illustration, Fig. 6 shows transformation of several typical clustering regions into mesodomains. Supposing that only those subdomains with $f_{loc,eff}^v = 40\%$ meet the above two criteria, then they will be transformed into mesodomains at the applied stress level. The RHS sketch of Fig. 6 displays the mesodomain distribution.

Given the volume fraction of the mesodomains, P_{ms} , and $f_{loc,eff}^v$ for the mesodomains, the local particle volume fraction for the ‘matrix’ f_{m}^v can be derived as

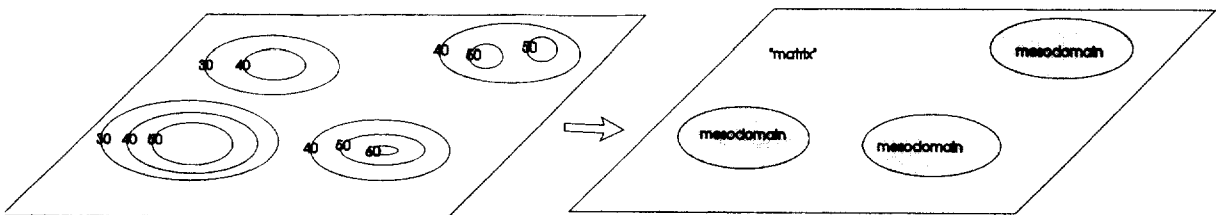


Fig. 6. Morphology of area contours and mapped mesodomains.

$$f_{\text{mt}}^{\text{v}} = \frac{f_{\text{v}}^{\text{c}} - f_{\text{loc,eff}}^{\text{v}} P_{\text{ms}}}{1 - P_{\text{ms}}} \quad (7)$$

in which f_{v}^{c} is the particle volume fraction of the composite. The material properties for the mesodomains and ‘matrix’ can be obtained based on $f_{\text{loc,eff}}^{\text{v}}$ for the mesodomains and f_{mt}^{v} for the ‘matrix’, respectively. Since $f_{\text{loc,eff}}^{\text{v}}$ generally is higher than the real f_{loc} in the clustering regions (see eqn (1)), f_{mt}^{v} will be slightly less than the real particle volume fraction in the area excluding the mesodomains. This makes sense from the local stress-concentration point of view, since the average particle size in the area corresponding to ‘matrix’ is smaller than the average size for the composite. Experimental results of elastic modulus for a series of metal matrix composites with different particle volume fraction are generally available from manufacturers or from open literature (Mummery and Derby, 1991). The data can be used to extrapolate the local material properties of the mesodomains and the ‘matrix’.

Other shapes, such as ellipsoids, can be used in place of the circular mesodomains, depending on materials and their manufacturing process.

5. Summary

The inhomogeneous particle distribution of PMMCs and resulting possibility of inducing localized damage are characterized by a parameter, termed herein an effective local particle volume fraction, $f_{\text{loc,eff}}^{\text{v}}$. The $f_{\text{loc,eff}}^{\text{v}}$ area contour plot for a representative micrograph displays the morphology and degree of the clustering distribution in the PMMCs. A stress-flaw size diagram is constructed based on experimental results for a PMMC, showing the dependence of localized damage region size on the applied stress amplitude.

The mesodomain simulation of inhomogeneous PMMCs is intended to facilitate the description of the localized damage and prediction of the saturated local damage life. Based on this methodology, the clustering regions of an inhomogeneous PMMC accommodating localized damage are simulated by mesodomains, subdomains of homogeneous medium and homogeneously distributed damage. The domain surrounding the clustering regions is then transformed into a homogeneous ‘matrix’, free of local damage. The mesodomain size is determined by the transition condition from damage localization to damage globalization (e.g., long crack growth) displayed in the stress-flaw diagram for the PMMC. The mesodomain location is identified by mapping the same size clustering regions of the highest $f_{\text{loc,eff}}^{\text{v}}$ value in the area contour plot of a representative micrograph of the composite.

The mesodomain simulation highlights an important feature of localized damage in inhomogeneous PMMCs—its dependence on both local material characteristic and applied stress, and embodies a combination of materials science and solid mechanics. Consequently, this mesodomain simulation enables application of Eshelby’s method as well as continuum damage mechanics.

Acknowledgements

The financial support provided by the Natural Sciences and Engineering Research Council of Canada is acknowledged. The authors also appreciate fruitful discussions with Dr D. Lloyd, Alcan International Ltd.

References

- Allen, R.J., Booth, G.S., Jutla, T., 1988. A review of fatigue crack growth characterization by linear elastic fracture mechanics (LEFM), Part I. *Fatigue Fract. Engng Mater. Struct.* 11, 45–69.
- Allison, J.E., Jones, J.W., 1993. In: Suresh, S., Mortensen, Needleman, A. (Eds.). *Fundamentals of Metal Matrix Composites*. Butterworth-Heinemann, pp. 269–294.
- Bazant, Z., 1997. Scaling of quasibrittle fracture: asymptotic analysis. *Int. J. Fract.* 83, 190–240.
- Brockenbrough, J., Hunt, W., Richmond, O., 1992. A reinforced material model using actual microstructure geometry. *Scripta Metal. Mater.* 27, 385–390.
- Chaboche, J.L., 1988. Continuum damage mechanics: part I—general concepts. *ASME J. Appl. Mech.* 55, 59–72.
- Clyne, T., Withers, P., 1993. *An Introduction to Metal Matrix Composites*. Cambridge University Press, Cambridge.
- Corbin, S.F., Wilkinson, D.S., 1994. Influence of matrix strength and damage accumulation on the mechanical response of a particulate metal matrix composite. *Acta Metal. Mater.* 42, 1329–1335.
- Costanzo, F., Boyd, J., Allen, D., 1996. Micromechanics and homogenization of inelastic composite materials with growing cracks. *J. Mech. Phys. Solids* 44, 330–370.
- Davidson, D.L., 1991. Fracture characteristics of Al-4Pct Mg mechanically alloyed with SiC. *Metal. Trans. A*. 18A, 2115–2138.
- El Haddad, M.H., Topper, H., Smith, K.N., 1979. Prediction of non-propagating cracks. *Engng Fract. Mech.* 11, 573–584.
- Flom, Y., Arsenault, J., 1989. Effect of particle size on fracture toughness of SiC/Al composite materials. *Acta Metal.* 37, 2413–2423.
- Haritos, G.K., Hager, J.W., Amos, A.K., Salakind, M.J., Wang, A.S.D., 1988. Mesomechanics: the microstructure-mechanics connection. *Int. J. Solids Struct.* 24, 1081–1096.
- Hild, F., Larsson, P.-L., Leckie, F.A., 1996. Localization due to damage in two-direction fiber-reinforced composites. *ASME J. Appl. Mech.* 63, 321–325.
- Hoshide, T., Furuya, H., Nagase, Y., Yamada, T., 1984. Fracture mechanics approach to evaluation of strength in sintered silicon nitride. *Int. J. Fract.* 26, 229–239.
- Iwan, W.D., 1967. On a class of models for the yielding behaviour of continuous and composite systems. *ASME J. Appl. Mech.* 34, 612–617.
- Kachanov, L.M., 1958. Time of the rupture under creep conditions. *Izv. Akad. Nauk., SSR, Otd. Tekh. Nauk*, Nr. 8, 26–31.
- Kitagawa, H., Takahashi, S., 1976. Applicability of fracture mechanics to very small cracks or cracks in early stage. *Proceedings of Second International Conference on Mechanical Behaviour of Materials*. Boston, MA, pp. 609–631.
- Krajcinovic, D., Mastilovic, S., 1995. Some fundamental issues of damage mechanics. *Mech. Mater.* 21, 217–230.
- Lemaitre, J., 1986. Local approach of fracture. *Engng Fract. Mech.* 22, 523–537.
- Ladeveze, P., Allix, O., Cluzel, C., 1993. Damage modelling at the macro- and meso-scales for 3D composites. *Damage In Composite Materials*. Elsevier Science, Netherlands.
- Lemaitre, J., 1986. Local approach of fracture. *Engng Fract. Mech.* 25, 523–537.
- Levy, A., Papazian, J.M., 1991. Elastoplastic finite element analysis of short-fiber-reinforced SiC/Al composites: effects of thermal treatment. *Acta Metall. Mater.* 39, 2255–2261.
- Lewandowski, J., Liu, C., Hunt, W., 1989. Effect of Matrix microstructure and particle distribution on fracture of aluminum metal matrix composite. *Mater. Sci. Engng A107*, 241–255.
- Li, C.-S., 1990. On mesomechanics of small cracks. *Bulletin of Taiyuan University* 21, 240–248.
- Li, C.-S., Ellyin, F., 1995a. On crack phases of particulate-reinforced metal matrix composites. *Fatigue Fract. Engng Mater. Struct.* 18, 1099–1109.
- Li, C., Ellyin, F., 1995b. Short crack growth behaviour in a particulate-reinforced aluminum composite. *Metall. Mater. Trans.* 26A, 3177–3182.
- Li, C.-S., Ellyin, F., 1996. Fatigue damage and its localization in particulate metal matrix composites. *Mater. Sci. and Eng.* 214A, 115–121.
- Liu, H.W., Liu, D., 1982. Near threshold fatigue crack growth behaviour. *Scripta Metall.* 16, 595–600.
- Lloyd, D.J., 1991. Aspects of fracture in particulate reinforced metal matrix composites. *Acta Metall.* 39, 59–71.
- Lloyd, D.J., 1995. Factors influencing the tensile ductility of melt processed particle reinforced aluminum alloys. In:

- Lewandowski, J., Hunt, W., Jr. (Eds.). Proceedings of Symposium of Intrinsic and Extrinsic Fracture Mechanisms. TMS, pp. 39–47.
- Mochida, T., Taya, M., Lloyd, D.J., 1991. Fracture of particles in a particle/metal matrix composite under plastic straining and its effect on the Young's modulus of the composite. *Mater. Trans. JIM* 32, 931–942.
- Mummery, P., Derby, B., 1991. The influence of microstructure on fracture behaviour of particulate-reinforced metal matrix composites. *Mater. Sci. Eng.* 135A, 221–224.
- Pilkey, A.K., Fowler, J.P., Worswick, M.J., Burger, G., Lloyd, D.J., 1990. Characterizing particle distribution in model aluminum alloy systems. *Microstructure Science* 22, 329–334.
- Pragnell, P.R., Barnes, S.J., Roberts, S.M., Withers, P.J., 1996. The effect of particle distribution on damage formation in particulate reinforced metal matrix composites deformed in compression. *Mater. Sci. and Engng* 220A, 41–56.
- Shang, J., Ritchie, R., 1988. On the particle size dependence of fatigue crack propagation threshold in SiC-particle-reinforced aluminum alloy composites: role of crack closure and crack trapping. *Acta Metall.* 17, 2267–2278.
- Spitzig, W.A., Smelser, R.E., Richmond, O., 1988. The evaluation of damage and fracture in iron compacts with various initial porosities. *Acta Metall.* 36, 1201–1209.
- Suresh, S., Ritchie, R.O., 1984. Propagation of short cracks. *Int. Metals Rev.* 29, 445–475.